Generation of a common innate lymphoid cell progenitor requires interferon regulatory factor 2

Yohei Okubo[1,2], Shigeo Tokumaru[1,2], Yuta Yamamoto[1,2], Shin-ichi Miyagawa[2], Hideki Sanjo[1] and Shinsuke Taki[1]

[1]Department of Molecular and Cellular Immunology, Shinshu University School of Medicine, Matsumoto 390-8621 Japan

[2]Department of Surgery, Shinshu University School of Medicine, Matsumoto 390-8621 Japan

Corresponding author: Shinsuke Taki, Ph.D., Department of Molecular and Cellular Immunology, Shinshu University School of Medicine, 3-1-1 Asahi, Mastumoto 390-8621 Japan

E-mail address: takishin@shinshu-u.ac.jp

TEL: +81-263-37-2610, FAX: +81-263-37-2613

Running title: IRF-2 in ILC development

Total 36 pages, 6 figures

ABSTRACT

Innate lymphoid cells (ILCs), composed of heterogeneous populations of lymphoid cells, contribute critically to immune surveillance at mucosal surfaces. ILC subsets develop from common lymphoid progenitors through stepwise lineage specification. However, the composition and temporal regulation of the transcription factor network governing such a process remain incompletely understood. Here we report that deletion of the transcription factor interferon regulatory factor 2 (IRF-2), known also for its importance in conventional NK cell maturation, resulted in an impaired generation of ILC1, ILC2 and ILC3 subsets with lymphoid tissue inducer-like (LTi) cells hardly affected. In IRF-2-deficient mice, PD-1^{hi} ILC precursors (ILCPs) that generate these three ILCs but not LTi cells were present at normal frequency, while their subpopulation expressing high amounts of PLZF, another marker for ILCPs, was severely reduced. Notably, these IRF-2-deficient ILCPs contained normal quantities of PLZF-encoding *Zbtb16* messages, and PLZF expression in developing invariant NKT cells within the thymus was unaffected in these mutant mice. These results point to a unique, cell-type selective role for IRF-2 in ILC development, acting at a discrete step critical for the generation of functionally competent ILCPs.

INTRODUCTION

Innate lymphoid cells (ILCs) constitute a heterogeneous lymphocyte population, locating mainly in skin, lung and liver as well as intestinal lamina propria (LP), where their effector functions contribute critically to a rapid protection against pathogen infection and tissue damages (1-3). ILCs are, similarly to helper T cells, classified into three major subpopulations, based on cytokine species they produce and transcription factor dependence; T-bet-dependent group 1 ILCs (ILC1s) producing IFN-γ, RORα- and GATA3-dependent ILC2s producing IL-5 and IL-13, and RORγt-dependent ILC3s producing IL-17 and IL-22. Lymphoid tissue inducers (LTis) in fetuses and LTi-like cells in adults are also members of the ILC3 subset and play a unique role, unlike other ILC3s, in secondary lymphoid organ development and tissue homeostasis (1,3,4).

All ILCs as well as conventional NK (cNK) cells develop from common lymphoid progenitors (CLPs) present in the fetal liver and adult bone marrow (BM). CLPs undergo progressive lineage-restricting events leading ultimately to the generation of immediate precursors for individual ILC subsets (3,5-8). Thus, along the ILC developmental pathway, CLPs develop first into the earliest precursor for cNK cells as well as all ILCs, termed αLP, that is positive for surface α4β7 integrin. αLP develop next into the common helper innate lymphoid cell progenitor (CHILP) that is $\alpha4\beta7^{+}FLT3^{-}CD25^{-}$ and generates all ILCs but not cNK cells. The CHILP population

contains PD-1^{hi} subpopulation called innate lymphoid cell precursor (ILCP) that has lost the developmental potential to LTi-like cells but retains those for ILC1, ILC2 and ILC3 cells. Intensive studies in recent years identified multiple transcription factors such as GATA3, NFIL3, TOX and TCF-1 critically important for the transition from CLP to its downstream CHILP stages (7,9-16). In contrast, although ILCP was shown to express the transcription factor PLZF encoded by the *Zbtb16* gene (6,7,16,17), little is known as to how CHILP to ILCP transition is regulated and what molecules are required for the step.

We and others showed previously that the transcription factor interferon regulatory factor 2 (IRF-2) was required for cNK cell maturation in BM and thus IRF-2 deficiency resulted in the arrest at the immature CD11b^{-}CD27^{+} stage (18,19). cNK cells were reported in the past to require the transcription factors NFIL3, TOX, Id2, ETS-1 and T-bet in addition to IRF-2 for their development and maturation (20-25). All of these factors were recently shown to be involved also in the development of one or multiple ILC subsets (9,10,16,26-28), while it was not known if IRF-2 contributes to ILC development. In this study, we found that IRF-2-deficient (*Irf2*$^{-/-}$) mice exhibited deficiencies in multiple ILC subsets. IRF-2 was dispensable for the generation of CHILPs and its downstream ILCPs (PD-1^{hi} CHILPs) but required for ILCP competence,

in part, through promoting PLZF expression. Our data here uncovered a previously unrecognized function of IRF-2 critical at a unique discrete step in the early development of ILCs.

METHODS

Mice

Irf2$^{-/-}$, *Irf2*$^{-/-}$*Rag1*$^{-/-}$ and *Irf2*$^{-/-}$*Ifnar1*$^{-/-}$ mice were described previously (29). *Rorc(γt)*$^{+/gfp}$ mice (kindly provided by Profs. D. Littman and A. Yoshimura) and mouse H-2K promoter-human *BCL2* transgenic mice (kindly provided by Dr. J. Domen and Prof. K. Ikuta) were described previously (30). Since we did not observe any significant difference between wild-type and *Irf2*$^{+/-}$ mice, we used littermates with either of these two genotypes as control mice for *Irf2*$^{-/-}$ mice without discrimination, unless otherwise stated. *Irf2*$^{-/-}$ mice were backcrossed to the C57BL/6J background more than 10 times and have since been maintained through sister-brother mating in a room under strict SPF condition in the Division of Animal Research, Shinshu University and used at 8-12 weeks of age. Compound mutant animals were generated by crossing these *Irf2*$^{-/-}$ mice with other mutant animals such as *Rag1*$^{-/-}$, *Ifnar1*$^{-/-}$, *Rorc(γt)*$^{+/gfp}$ and human *BCL2* transgenic mice, which had been maintained in the same room on the same diet as those for *Irf2*$^{-/-}$ mice. All animal experiments were preapproved by the Division of Animal Research of Shinshu University (#250019, #250057, #270057, #280070) and performed in accordance with the Regulation for Animal Experimentation of Shinshu University.

Isolation of lymphoid cells

Isolation of lamina propria cells were carried out as described (31). The guts were removed of Peyer's patches, cut open into pieces, incubated for 30 min at 37 ^{o}C in PBS containing 5mM EDTA and 2mM DTT and washed for 30 sec with PBS intensely three times. Gut pieces were washed with PBS on a cell strainer to remove intraepithelial lymphocytes, cut into pieces of 1mm in length and incubated for 60 min at 37 ^{o}C in RPMI1640 medium containing collagenase type IV (0.5mg/ml; SIGMA-ALDRICH) and DNase Ⅰ(50U/ml; Wako), washed and strained through nylon mesh. Cells were suspended in 40% Percoll (GE Health science) and overlaid on 80% Percoll. Lymphoid cells were collected from the 80/40 interphase after centrifuge. For the isolation of liver and lungs cells, these organs were washed with PBS to remove blood, minced and incubated for 30 min at 37 ^{o}C in HANKS' salt solution containing collagenase type IV (0.5mg/ml;) and DNase Ⅰ(50U/ml; Wako), followed by straining through a cell strainer. Lymphoid cells were collected using Percoll as above. Isolated intestinal lymphoid cells were cultured *in vitro* for 4 hours in the presence of PMA (50 ng/ml), ionomycin (500 mg/ml), and GoldiStop (BD Science) for the last 3 hours. Cultured cells were stained to identify ILC2s, fixed and stained intracellularly with PE anti-IL-5 (BioLegend) as below.

Flow cytometry and cell sorting

Fluorochrome-conjugated antibodies used in this study are listed below. Single cell suspensions obtained from various organs were treated with anti-CD16/32 antibody prepared in house to block Fc receptors and stained with Fixable Viability Dye eFluor 780 (Thermo Fischer Scientific) and fluorochrome-conjugated antibodies as described (31). Data were acquired using the FACS Canto II (BD Biosciences) or FACS Celesta (BD Biosciences) flow cytometer, except for those in Fig. 2 using the FC500 flowcytometer (Beckman Coulter). Data analysis was performed by Kaluza software (Beckman Coulter). Gating strategy used to identify ILC subsets and their progenitors was as follows. After excluding doublets and dead cells (with propidium iodide or Fixable Viability Dye eFlour 780), dot plots were gated on $CD45^+$ white blood cells for further analyses. For ILC subsets in RAG1-sufficient animals, only $CD45^+CD3^-$ cells were analyzed further. When BM cells were analyzed, lineage cocktail containing antibodies against CD3, CD11b, CD11c, CD19, B220, Ly6G/C, TCRβ, TCRγδ, NK1.1 and Ter119 were used to exclude lineage marker-positive (Lin^+) cells, and $CD45^+Lin^-$ cells were analyzed further. To analyze and collect CHILPs and their subsets, which are known to be $CD25^-$, anti-CD25 was included in lineage cocktail.

Fluorochrome-conjugated antibodies against following antigens were used. CD3 (145-2C11), CD8α (53-6.7), CD19 (1D3), Ly6G (1A8), CD11c (HL3), CD49a (HMα1), NK1.1 (PK136) from BD Pharmingen; CD11c (N418), CD45.2 (104), DX5 (DX5), TCRβ (H57-597), TER119 (TER-119), CD127 (A7R34), NK1.1 (PK136), PD-1 (J43), CD4 (RM4-5), KLRG1 (2F1), B220 (RA3-6B2), CD11b (M1/70), CD45.1 (A20), CD45 (30-F11), cKit (2B8), SCA1 (D7) from eBioscience; CD4 (RM4-5), CD45.2 (104), NK1.1 (PK136), TCRγδ (GL3), Ly6G/C (RB6-8C5), CCR6 (29-2L17), TER119 (TER-119), TCRβ (H57-597), FLT3 (A2F10), CD3 (145-2C11), CD11c (N418), CD127 (A7R34), cKit (ACK2), CD4 (RM4-5), α4β7 (DATK32) from BioLegend; CD4 (RM4-5), CD11b (M1/70), CD45.1 (A20), B220 (RA3-6B2), CD3 (145-2C11), CD11c (N418), CD127 (A7R34), cKit (ACK2), NK1.1 (PK136) from TONBO; T1/ST2 (DJ8) from MD Bioscience. PE-Cy7- and BV421-streptavidins from BD Pharmingen were also used. Antibodies to PLZF (R17-809; BD Pharmingen, 9E12; BioLegend) were used for intracellular staining with FoxP3/Transcription Factor Fixation/Permeabilization Concentrate and Diluent (eBioscience) as instructed by the supplier. To identify invariant NKT cells, dimeric mouse CD1d-IgG1 fusion protein (DimerX; BD Pharmingen) was loaded with α-galactosylceramide (Funakoshi) and used for staining according to the instruction by the supplier. For cell sorting, Lin^- cells were collected

using the AutoMACS (Miltenyi Biotec), followed by staining with antibodies against CD45 and various markers to sort on a FACS Aria III (BD Biosciences). For intracellular cytokines, Fixation/Permiabilization Solution Kit (BD Biosciences) was used according to the instruction by the supplier.

Radiation bone marrow chimeras

Radiation BM chimeras were prepared as described (29). Irradiated (9.5Gy) B6-Ly5.1 recipient mice were transferred *i.v.* with red blood cell-lysed bone marrow cells (1×10^7) and analyzed 8-9 weeks later.

Real-time RT-PCR

RT-PCR analyses were performed as described (31). Briefly, total RNA was isolated from sorted cells using RNeasy Kit (Quiagen), and converted to cDNA. Real-time PCR was performed using SYBR Premix Ex Taq II (TaKaRa) and Thermal Cycler Dice Real Time System (TaKaRa) according to the manufacturer's instruction. Amounts of specific mRNA were normalized to those of *Gapdh* mRNA. The following PCR primers were used: *Zbtb16* Forward, 5'-CAGTTTGCGACTGAGAATGCA-3'; *Zbtb16* Reverse, 5'-TCCTTTGAGAACTGGGCACC-3'; *Irf2* Forward,

5’-CCAGGGCTAAAGTGGCTGAA-3’; *Irf2* Reverse,

5’-AGAGCGGAGCATCCTTTTCC-3’; *Gapdh* Forward,

5’-GATGGGTGTGAACCACGAGA-3’; *Gapdh* Reverse,

5’-GCCCTTCCACAATGCCAAAG-3’.

Statistical analysis

Statistical analyses were performed using GraphPad Prism Software by unpaired t test for statistical significance.

RESULTS

Requirement for IRF-2 in the development of cNK cells, ILC1s and ILC3s.

To determine whether IRF-2 plays roles in ILC development, we investigated $CD3^-$ lymphoid cells in the small intestine in *Irf2*$^{-/-}$ mice. In line with previous reports (18,32), cNK cells, defined as $NKp46^+NK1.1^+CD127^-$, were defective in these mice (Fig.1A, C). Absolute numbers of $NK1.1^+CD127^+$ cells, representing ILC1s, were also two- to three-fold reduced in *Irf2*$^{-/-}$ mice in comparison with those in control mice (Fig.1C). Furthermore, $NKp46^+$ ILC3s, another ILC population defined as $NKp46^+NK1.1^-CD127^+$, were several-fold less abundant in *Irf2*$^{-/-}$ mice than in control mice (Fig.1C). In comparison to cNK, ILC1s and $NKp46^+$ ILC3s, a less severe, yet significant, reduction was seen for $NKp46^-CD4^-CD127^+$ ($NKp46^-CD4^-$ ILC3), a minor ILC3 subset (Fig.1B), and the reduction of $NKp46^-CD4^+CD127^+$ (LTi-like) cells, the other minor ILC3 subset (Fig.1B), was even more marginal in the absence of IRF-2 (Fig.1C). Consistent with this observation, we found no significant reduction of the numbers of Peyer's patches (unpublished observations). ILC2s ($NKp46^-KLRG1^+CD127^+$) seemed to be unaffected in *Irf2*$^{-/-}$ mice (Fig.1B, C). These observations suggested that IRF-2 was involved critically in ILC1 and $NKp46^+$ ILC3 development and less so in other ILC populations. Since additional null mutations in the *Ifnar1* loci in *Irf2*$^{-/-}$ mice did not restore the numbers of NK, ILC1 and $NKp46^+$ ILC3

cells (P>0.5 for 3 pairs of *Irf2*$^{-/-}$ and *Irf2*$^{-/-}$*Ifnar1*$^{-/-}$ mice, data not shown), IRF-2 appeared to regulate ILC generation independently of its attenuator function for type I interferon signals.

ILC2s as well as ILC1s and ILC3s but not LTi-like cells required IRF-2 on the RAG1-deficient background

Taking advantage of mutant mice harboring green fluorescent protein reporter DNA in the exon 1γt in the *Rorc* gene (*Rorc*$^{gfp/+}$ mice (33)), we further examined ILC development in *Irf2*$^{-/-}$ mice. The animals used in this series of examinations were on the *Rag1*$^{-/-}$ background for excluding the influence, if any, of T and B cells. Again, NKp46^{+} ILC3s (NKp46^{+}RORγt^{+}), ILC1s (NKp46^{+}NK1.1^{+}CD127^{+}RORγt^{-}) and cNK cells (NKp46^{+}NK1.1^{+}CD127^{-}RORγt^{-}) were clearly reduced in *Irf2*$^{-/-}$*Rag1*$^{-/-}$*Rorc*$^{gfp/+}$ mice (Fig.2A. C). LTi-like cells (NKp46^{-}KLRG1^{-}RORγt^{+}CD4^{+}, Fig.2A) were present at normal frequencies, while the reduction of NKp46^{-}CD4^{-} ILC3s (NKp46^{-}CD4^{-}RORγt^{+}) was observed consistently in these mice (Fig2A, C). It was notable that the frequencies and absolute numbers of ILC2s (NKp46^{-}KLRG1^{+}) were several times lower in *Irf2*$^{-/-}$*Rag1*$^{-/-}$*Rorc*$^{gfp/+}$ mice than in control *Rag1*$^{-/-}$*Rorc*$^{gfp/+}$ mice (Fig.2B, C). In addition, the numbers of intestinal ILC2s in *Irf2*$^{-/-}$*Rag1*$^{-/-}$ and control *Rag1*$^{-/-}$ mice

without the *gfp* insertion were also significantly different ($p<0.01$; 1.01 +/- 0.51 $x10^5$ and 2.53 +/- 1.10 x 10^5 cells, respectively, n=3 for each genotype). These observations did not fully agree with those observed in the RAG1-sufficient background (Fig.1C) and implied a possibility that the presence of T and/or B cells hindered the influence of IRF-2 deficiency on ILC2 development. In support of impaired ILC2 development in the absence of IRF-2, we found that immature ILC2s in the BM ($Lin^-T1/ST2^+SCA1^+KLRG1^-$ (34)) were less abundant in RAG1-sufficient *Irf2*$^{-/-}$ mice than in control (Fig.3A, B). Compensation of impaired ILC2 development in *Irf2*$^{-/-}$ mice possibly by T and/or B cells seemed to occur in the periphery. Furthermore, although we could not reliably measure IL-22 production by IRF-2-deficient ILC3s due to their paucity, IL-5 and IL-13 production by IRF-2-deficient and control ILC2s was comparable (62.6+/-2.3% vs. 62.8+/-0.36%, respectively for IL-5, and 29.9+/-14.4% vs. 25.5%+/-3.1%, respectively for IL-13; mean +/- SD of two independent experiments), suggesting that IRF-2 contributed to homeostasis rather than effector functions of ILCs.

ILC deficiency occurred systemically due to the defect(s) in ILC progenitors in BM.

According to the unique tissue distribution of ILC populations, the liver and lung harbored high numbers of ILC1s and ILC2s, respectively (28,35). We hence examined

hepatic ILC1s and pulmonary ILC2s in *Irf2*$^{-/-}$*Rag1*$^{-/-}$ mice. The numbers of ILC1s (NKp46^{+}NK1.1^{+}CD49a^{+}DX5^{-} (36)) and cNK cells (NKp46^{+}NK1.1^{+}CD49a^{-}DX5^{+}) in the liver were around 5- and 20- fold reduced, respectively, compared with those in control *Rag1*$^{-/-}$ mice (Fig.4A, C). In the lung, cNK cells (NKp46^{+}NK1.1^{+}CD127^{-}) and ILC2s (KLRG1^{+}CD127^{+}) were 50- and 3-times less in *Irf2*$^{-/-}$*Rag1*$^{-/-}$ than in control *Rag1*$^{-/-}$ mice, respectively (Fig.4B, C). These observations indicated that IRF-2 deficiency affected ILC populations not only in the small intestine but also in other locations, pointing to a potential defect in hematopoietic progenitors for ILCs.

To determine whether the ILC deficiency was cell intrinsic or not, we transferred BM cells from *Irf2*$^{-/-}$*Rorc*$^{gfp/+}$ or control *Rorc*$^{gfp/+}$ mice into irradiated CD45.1 (Ly5.1) mice. Usually, to examine the repopulation potential for BM hematopoietic progenitors, control BM cells and those to be tested are mixed and transferred to establish mixed BM chimeras. However, as demonstrated previously (37), IRF-2-deficient hematopoietic stem cells were inferior to wild-type counterparts in repopulating in radiation BM chimeras under competitive conditions, hampering us from employing mixed BM chimeras for this purpose. Even in the conventional non-competitive BM chimeras, however, we observed that IRF-2-deficient BM cells yielded less NKp46^{+} ILC3s (Supplementary Fig.1). We also observed that LTi-like NKp46^{-}CD4^{+} ILC3s were not

significantly affected and CD4^{-}NKp46^{-} ILC3s and ILC2s reduced marginally but significantly. It was also obvious that RORγt^{-}NKp46^{+}NK1.1^{+} cells, representing a mixed population of ILC1s and cNK cells, were less abundant in IRF-2-deficient than control chimeras. Based on these observations, we infer that ILC-related phenotypes in *Irf2*$^{-/-}$ mice were intrinsic to BM-resident hematopoietic cells.

PD-1^{hi} CHILP generation was unaffected in *Irf2*$^{-/-}$ mice

With respect to IRF-2 actions in cNK cells and ILCs, we noted that upon enforced expression of a human *BCL2* transgene under the control of murine MHC class I promoter (30), cNK cell deficiency in the small intestine in *Irf2*$^{-/-}$ mice were rescued substantially, but ILC1, ILC2, NKp46^{+} ILC3 and NKp46^{-} ILC3 deficiencies not at all (Fig.5A). This observation suggested that IRF-2 deficiency affected ILC development after divergence between cNK and ILC lineages. We next carried out flow cytometry on BM cells to examine progenitors for ILCs in *Irf2*$^{-/-}$ mice, and found that the whole CHILP population (Lin^{-}c-kit^{+}CD127^{+}CD25^{-}FLT3^{-}α4β7^{hi}, Fig.5B) was not reduced, if slightly enlarged, in *Irf2*$^{-/-}$ mice as compared with those in control mice (Fig.5C). ILCPs defined as CHILPs expressing high amounts of PD-1 (PD-1^{hi} CHILPs) (7) were also as abundant in *Irf2*$^{-/-}$ mice as in control. In contrast, PD-1$^{lo/-}$ CHILPs were about

2-fold more frequent in *Irf2*$^{-/-}$ mice than in control (Fig.5B, C). The enlargement of PD-1$^{lo/-}$ CHILP population were accounted for partly by increase of CCR6^{+}CD4^{+} subpopulation that likely represented LTi-like cell progenitors (17) (Supplementary Fig.2A, B).

ILCPs in *Irf2*$^{-/-}$ mice lacked the PLZF-expressing subpopulation.

PLZF was another important marker for ILCPs (6,7,16). Accordingly, intracellular staining of PLZF proteins showed that the great majority of PD-1^{hi} CHILPs were PLZF^{hi} in control mice. Noticeably, in contrast, *Irf2*$^{-/-}$ mice lacked the PLZF^{hi} population in PD-1^{hi} CHILPs (Fig.6A, B), suggesting that IRF-2 was required for PLZF expression. To examine the transcriptional activation by IRF-2 of the *Zbtb16* gene that encoded PLZF, CLPs (Lin^{-}CD127^{+}c-kit^{+}Flt3^{+}α4β7^{-}), whole CHILPs and PD-1^{hi} CHILPs were sorted separately from BM cells, and quantitative RT-PCR was carried out for *Zbtb16* messages. In agreement with a previous report (6,7,16), CLPs in control mice expressed only low amounts of *Zbtb16* messages, and developmental progression to the CHILP stage was accompanied with several hundred-fold elevation (Fig.6C). Unexpectedly, PD-1^{hi} CHILPs from *Irf2*$^{-/-}$ mice expressed as much *Zbtb16* messages as those from control mice. Significantly less *Zbtb16* messages in whole CHILP from

Irf2$^{-/-}$ mice than from control were due probably to the higher percentages of PD-1$^{lo/-}$ cells, which would express less *Zbtb16* messages than PD-1^{hi} cells, among CHILPs in *Irf2*$^{-/-}$ mice than in control (see Fig.5B, C). These observations suggested that IRF-2 was dispensable for the transcription of the *Zbtb16* gene but critical for PLZF protein expression. Unlike in PD-1^{hi} CHILPs, however, developing invariant NKT (iNKT) cells in the thymus, another cell type known to express PLZF, exhibited an identical developmentally regulated PLZF expression pattern (38) in *Irf2*$^{-/-}$ and control mice, wherein NK1.1^{-} iNKT cells representing cells of earlier developmental stages expressed high amounts of PLZF while NK1.1^{+} more mature iNKT cells expressed less PLZF than NK1.1^{-} iNKT cells (Fig.6E). Thus IRF-2 deficiency did not affect PLZF expression in developing iNKT cells in the thymus, pointing to a unique requirement for IRF-2 in PLZF expression selectively during CHILP to ILCP transition. We observed, rather unexpectedly, that *Irf2* gene expression levels were constant as ILC development advanced from CLP to ILCP stages (Fig.6D), indicating that the presence of IRF-2 alone was not sufficient to determine the timing of PLZF expression during ILC development.

DISCUSSION

Sequential restriction of lineage potential underlies the commitment of multipotential hematopoietic progenitors to distinct cell lineages. As for the development of diverse ILC subsets, CHILPs were generated from CLPs through suppressing the potential to generate T, B and cNK cells. Whereas multiple transcription factors were associated with this CHILP generation process (7,9-16), much less numbers of factors have been identified to be involved in the next developmental step where CHILPs become ILCPs through losing the potential to develop into LTi-like cells but retaining that for ILC1, ILC2 and ILC3 cells. Our current study has revealed that generation of functionally competent ILCPs required IRF-2 at this less-well-studied developmental step. The reduction of ILC1, ILC2 and ILC3 with overtly unaffected LTi-like cell numbers in *Irf2*$^{-/-}$ mice was coincide with what would be expected if ILCPs rather than CHILPs were impaired. The CHILP population in BM in *Irf2*$^{-/-}$ mice was rather enlarged due to the accumulation of its PD-1$^{lo/-}$ subset including CCR6^{+} cells that reportedly represented progenitors committed towards the LTi-like cell lineage (17). For as yet unknown reasons, the increase of CCR6^{+} CHILPs in BM did not necessarily result in the increase of LTi-like cells in the intestine. These observations suggested, nevertheless, that generation of LTi progenitors was accelerated in the absence of IRF-2, implicating a

negative impact of IRF-2 on this process. The differential rescue by a human *BCL2* transgene of cNK from other ILCs in *Irf2*$^{-/-}$ mice indicated that the major developmental defect in cNK cells in *Irf2*$^{-/-}$ mice was mechanistically distinct from that in ILCs, occurring after cNK cell precursors diverged from the main stream ILC developmental pathway. In support of this prediction, the major arrest during cNK development was previously shown to occur relatively late in the BM at the transition from CD11b^{-}CD27^{+} to CD11b^{+}CD27^{+} immature cNK cells at least partly due to accelerated apoptosis (18,19). These observations above altogether suggested that IRF-2 participates in different developmental stages for distinct non-adaptive lymphocyte lineages, as do some other transcription factors such as T-bet, ETS-1 and NFIL3.

Murine ILCPs were defined as the PLZF^{hi} subpopulation of CHILPs (6,7,16) and those co-expressing high levels of PD-1 (7). In *Irf2*$^{-/-}$ mice, PD-1^{hi} CHILPs in the BM were present as frequently as those in control mice, indicating that IRF-2 was not essential for CHILPs to upregulate PD-1 expression. Notably, however, these PD-1^{hi} CHILPs in *Irf2*$^{-/-}$ mice lacked the PLZF^{hi} subpopulation. In accordance with a recent report (39), this indicated that PD-1^{hi} CHILPs were generated from their PD-1$^{lo/-}$ precursors independently of PLZF expression. Given that PLZF itself was required for the development of ILC2s and liver ILC1s but apparently not intestinal ILC3s (6), the

failure of IRF-2-deficient CHILPs to express PLZF would alone not account for the reduction of intestinal ILC3s in *Irf2*$^{-/-}$ mice. Rather, we infer that in the absence of IRF-2, ILC progenitors could not advance efficiently to the stage where not only PLZF but also other yet to be identified molecules critical for ILC development were expressed. In addition, the increase of PD-1$^{lo/-}$ CHILPs, particularly their CCR6^{+}CD4^{+} subset that likely represent LTi-like cell progenitors (17), in *Irf2*$^{-/-}$ mice suggested that a skewed differentiation of ILC progenitors towards LTi-like cells is otherwise restricted by IRF-2.

Messages for IRF-2 were expressed already in the CLP stage as strongly as in CHILPs, and hence IRF-2 expression itself did not mark the boundary between the CHILP and ILCP stages. This finding raised a question as to how IRF-2 requirement appeared at the CHILP to ILCP transition. A possible scenario would be that a factor(s) that cooperatively works with IRF-2 begins to be expressed in CHILPs and initiates the IRF-2-dependent transcriptional program that ensures ILCP competence. In this regard, it would be noteworthy that a transcription factor called HCFC2 was recently shown to act as a critical component of IRF-2-mediated transcriptional machinery in peritoneal macrophages (40). In the absence of HCFC2, IRF-2 failed to bind to its cognate target DNA sequences and transactivate genes such as *Tlr3*, *Bcl11a* and *Csf1*. HCFC2 itself,

however, does not appear to be a plausible candidate since the *Hcfc2* gene was not found in the list of genes that exhibited differential expression in BM progenitors representing various stages of ILC development (16,39), wherein the *Pdcd1* and *Zbtb16* genes encoding PD-1 and PLZF, respectively, were readily identified. It is also possible that a gene(s) inhibiting IRF-2-mediated transcription is down-modulated as CHILPs differentiate to ILCPs. We expect that further studies would find a co-activator or co-repressor working together with IRF-2 among a multitude of genes reported to be upregulated or downregulated concomitantly with ILCP generation (7,16,39).

The presence of PD-1^{hi}PLZF^{lo} CHILPs expressing abundant *Zbtb16* messages in *Irf2*$^{-/-}$ mice indicated that the *Zbtb16* gene was not a direct target of IRF2-mediated transcriptional regulation. This was also supported by the apparently normal expression pattern for PLZF seen in developing iNKT cells in the thymus in *Irf2*$^{-/-}$ mice. It should be noted that PD-1^{hi}PLZF^{lo} CHILPs were present not only in *Irf2*$^{-/-}$ but also in control mice, yet at relatively low frequencies (see Fig.6A). This would point to a possibility that CHILPs expressing abundant *Zbtb16* message but only limited amounts of PLZF protein represent an intermediate stage between CHILPs and ILCPs. Interestingly, a PLZF^{lo} intermediate population functionally precedent to ILCPs was recently identified based on their *Tcf7-EGFP* reporter expression (39). More detailed study would, of

course, be necessary before concluding that these PD-1^{hi}PLZF^{dull} CHILPs abundantly seen in *Irf2*$^{-/-}$ mice represented indeed the intermediate population accumulated as a result of developmental arrest. However, we consider that *Irf2*$^{-/-}$ mice provide us with a unique experimental opportunity with which to get further insights into the order of and causative relationship among molecular events taking place during ILC development. Curiously, although the defects in ILC2 development in *Irf2*$^{-/-}$ mice were seen at the level of immature ILC2s in the BM, reduction of mature ILC2s in the intestine was apparent in RAG1-deficient but not sufficient *Irf2*$^{-/-}$ mice, implying a role for adaptive lymphocytes in the manifestation of the phenotypes by IRF-2-deficient ILC2s. As observed in this study, ILC2 numbers appeared to be elevated in the absence of adoptive lymphocytes as ILC2 numbers in *Rag1*$^{+/+}$ and *Rag1*$^{-/-}$ mice were 0.43 +/- 0.12 x 10^5 and 2.53 +/- 1.10 x 10^5 cells (n=3 for each genotype, Fig.1C and not depicted). These observations suggested that in the absence of adaptive lymphocytes, ILC2s might have bigger niches to fill up or alternatively be released from restraint by adaptive lymphocytes, resulting in additional rounds of proliferation. Such a presumptive expansion of ILC2s induced by the lack of adoptive lymphocytes might be less efficient in the absence of IRF-2 than in wild-type conditions. IRF-2 may thus potentially play roles, under specific conditions such as lymphopenia, in the homeostasis of ILC2s in the

peripheral lymphoid organs as well as in their early development.

In summary, the current study has uncovered a critical contribution by IRF-2 to the promotion of ILC development chiefly via supporting efficient generation of ILCPs, the event in which other transcription factors have hardly been known to act. Understanding how IRF-2 regulates its target gene expression at that developmental stage will help us dissect the gene regulatory network underlying ILC divergence.

Funding

This work was supported by a Grant-in-Aid for Scientific Research (C) (15K08529, 18K07170) to S.T. from The Ministry of Education, Culture, Sports, Science and Technology of Japan.

Acknowledgements

We thank Profs. Dan R. Littman and Akihiko Yoshimura for *Rorc*$^{gfp/+}$ mice and Dr. Jos Domen and Prof. Koichi Ikuta for human *BCL2* transgenic mice.

REFERENCES

1 Spits, H., Artis, D., Colonna, M., Diefenbach, A., Di Santo, J. P., Eberl, G., Koyasu, S., Locksley, R. M., McKenzie, A. N., Mebius, R. E., Powrie, F., and Vivier, E. 2013. Innate lymphoid cells--a proposal for uniform nomenclature. *Nat Rev Immunol* 13:145.

2 Diefenbach, A., Colonna, M., and Koyasu, S. 2014. Development, differentiation, and diversity of innate lymphoid cells. *Immunity* 41:354.

3 Artis, D. and Spits, H. 2015. The biology of innate lymphoid cells. *Nature* 517:293.

4 Eberl, G., Colonna, M., Di Santo, J. P., and McKenzie, A. N. 2015. Innate lymphoid cells. Innate lymphoid cells: a new paradigm in immunology. *Science* 348:aaa6566.

5 Klose, C. S., Flach, M., Mohle, L., Rogell, L., Hoyler, T., Ebert, K., Fabiunke, C., Pfeifer, D., Sexl, V., Fonseca-Pereira, D., Domingues, R. G., Veiga-Fernandes, H., Arnold, S. J., Busslinger, M., Dunay, I. R., Tanriver, Y., and Diefenbach, A. 2014. Differentiation of type 1 ILCs from a common progenitor to all helper-like innate lymphoid cell lineages. *Cell* 157:340.

6 Constantinides, M. G., McDonald, B. D., Verhoef, P. A., and Bendelac, A. 2014. A committed precursor to innate lymphoid cells. *Nature* 508:397.

7 Yu, Y., Tsang, J. C., Wang, C., Clare, S., Wang, J., Chen, X., Brandt, C., Kane, L., Campos, L. S., Lu, L., Belz, G. T., McKenzie, A. N., Teichmann, S. A., Dougan, G., and Liu, P. 2016. Single-cell RNA-seq identifies a PD-1(hi) ILC progenitor and defines its development pathway. *Nature* 539:102.

8 Ishizuka, I. E., Constantinides, M. G., Gudjonson, H., and Bendelac, A. 2016.

The Innate Lymphoid Cell Precursor. *Annu Rev Immunol* 34:299.

9 Yu, X., Wang, Y., Deng, M., Li, Y., Ruhn, K. A., Zhang, C. C., and Hooper, L. V. 2014. The basic leucine zipper transcription factor NFIL3 directs the development of a common innate lymphoid cell precursor. *Elife* 3:e04406.

10 Geiger, T. L., Abt, M. C., Gasteiger, G., Firth, M. A., O'Connor, M. H., Geary, C. D., O'Sullivan, T. E., van den Brink, M. R., Pamer, E. G., Hanash, A. M., and Sun, J. C. 2014. Nfil3 is crucial for development of innate lymphoid cells and host protection against intestinal pathogens. *J Exp Med* 211:1723.

11 Yagi, R., Zhong, C., Northrup, D. L., Yu, F., Bouladoux, N., Spencer, S., Hu, G., Barron, L., Sharma, S., Nakayama, T., Belkaid, Y., Zhao, K., and Zhu, J. 2014. The transcription factor GATA3 is critical for the development of all IL-7Ralpha-expressing innate lymphoid cells. *Immunity* 40:378.

12 Serafini, N., Klein Wolterink, R. G., Satoh-Takayama, N., Xu, W., Vosshenrich, C. A., Hendriks, R. W., and Di Santo, J. P. 2014. Gata3 drives development of RORgammat+ group 3 innate lymphoid cells. *J Exp Med* 211:199.

13 Seehus, C. R., Aliahmad, P., de la Torre, B., Iliev, I. D., Spurka, L., Funari, V. A., and Kaye, J. 2015. The development of innate lymphoid cells requires TOX-dependent generation of a common innate lymphoid cell progenitor. *Nat Immunol* 16:599.

14 Xu, W., Domingues, R. G., Fonseca-Pereira, D., Ferreira, M., Ribeiro, H., Lopez-Lastra, S., Motomura, Y., Moreira-Santos, L., Bihl, F., Braud, V., Kee, B., Brady, H., Coles, M. C., Vosshenrich, C., Kubo, M., Di Santo, J. P., and Veiga-Fernandes, H. 2015. NFIL3 orchestrates the emergence of common helper innate lymphoid cell precursors. *Cell Rep* 10:2043.

15 Yang, Q., Li, F., Harly, C., Xing, S., Ye, L., Xia, X., Wang, H., Wang, X., Yu, S., Zhou, X., Cam, M., Xue, H. H., and Bhandoola, A. 2015. TCF-1 upregulation identifies early innate lymphoid progenitors in the bone marrow. *Nat Immunol* 16:1044.

16 Seillet, C., Mielke, L. A., Amann-Zalcenstein, D. B., Su, S., Gao, J., Almeida, F. F., Shi, W., Ritchie, M. E., Naik, S. H., Huntington, N. D., Carotta, S., and Belz, G. T. 2016. Deciphering the Innate Lymphoid Cell Transcriptional Program. *Cell Rep* 17:436.

17 Ishizuka, I. E., Chea, S., Gudjonson, H., Constantinides, M. G., Dinner, A. R., Bendelac, A., and Golub, R. 2016. Single-cell analysis defines the divergence between the innate lymphoid cell lineage and lymphoid tissue-inducer cell lineage. *Nat Immunol* 17:269.

18 Taki, S., Nakajima, S., Ichikawa, E., Saito, T., and Hida, S. 2005. IFN Regulatory Factor-2 Deficiency Revealed a Novel Checkpoint Critical for the Generation of Peripheral NK Cells. *J Immunol* 174:6005.

19 Li, M. M., Bozzacco, L., Hoffmann, H. H., Breton, G., Loschko, J., Xiao, J. W., Monette, S., Rice, C. M., and MacDonald, M. R. 2016. Interferon regulatory factor 2 protects mice from lethal viral neuroinvasion. *J Exp Med* 213:2931.

20 Gascoyne, D. M., Long, E., Veiga-Fernandes, H., de Boer, J., Williams, O., Seddon, B., Coles, M., Kioussis, D., and Brady, H. J. 2009. The basic leucine zipper transcription factor E4BP4 is essential for natural killer cell development. *Nat Immunol* 10:1118.

21 Kamizono, S., Duncan, G. S., Seidel, M. G., Morimoto, A., Hamada, K., Grosveld, G., Akashi, K., Lind, E. F., Haight, J. P., Ohashi, P. S., Look, A. T., and

Mak, T. W. 2009. Nfil3/E4bp4 is required for the development and maturation of NK cells in vivo. *J Exp Med* 206:2977.

22 Aliahmad, P., de la Torre, B., and Kaye, J. 2010. Shared dependence on the DNA-binding factor TOX for the development of lymphoid tissue-inducer cell and NK cell lineages. *Nat Immunol* 11:945.

23 Yokota, Y., Mansouri, A., Mori, S., Sugawara, S., Adachi, S., Nishikawa, S., and Gruss, P. 1999. Development of peripheral lymphoid organs and natural killer cells depends on the helix-loop-helix inhibitor Id2. *Nature* 397:702.

24 Barton, K., Muthusamy, N., Fischer, C., Ting, C. N., Walunas, T. L., Lanier, L. L., and Leiden, J. M. 1998. The Ets-1 transcription factor is required for the development of natural killer cells in mice. *Immunity* 9:555.

25 Townsend, M. J., Weinmann, A. S., Matsuda, J. L., Salomon, R., Farnham, P. J., Biron, C. A., Gapin, L., and Glimcher, L. H. 2004. T-bet regulates the terminal maturation and homeostasis of NK and Valpha14i NKT cells. *Immunity* 20:477.

26 Klose, C. S., Kiss, E. A., Schwierzeck, V., Ebert, K., Hoyler, T., d'Hargues, Y., Goppert, N., Croxford, A. L., Waisman, A., Tanriver, Y., and Diefenbach, A. 2013. A T-bet gradient controls the fate and function of CCR6-RORgammat+ innate lymphoid cells. *Nature* 494:261.

27 Rankin, L. C., Groom, J. R., Chopin, M., Herold, M. J., Walker, J. A., Mielke, L. A., McKenzie, A. N., Carotta, S., Nutt, S. L., and Belz, G. T. 2013. The transcription factor T-bet is essential for the development of NKp46+ innate lymphocytes via the Notch pathway. *Nat Immunol* 14:389.

28 Zook, E. C., Ramirez, K., Guo, X., van der Voort, G., Sigvardsson, M., Svensson, E. C., Fu, Y. X., and Kee, B. L. 2016. The ETS1 transcription factor is required

for the development and cytokine-induced expansion of ILC2. *J Exp Med* 213:687.

29 Notake, T., Horisawa, S., Sanjo, H., Miyagawa, S., Hida, S., and Taki, S. 2012. Differential requirements for IRF-2 in generation of CD1d-independent T cells bearing NK cell receptors. *J Immunol* 188:4838.

30 Domen, J. and Weissman, I. L. 2003. Hematopoietic stem cells and other hematopoietic cells show broad resistance to chemotherapeutic agents in vivo when overexpressing bcl-2. *Exp Hematol* 31:631.

31 Sanjo, H., Tokumaru, S., Akira, S., and Taki, S. 2015. Conditional Deletion of TAK1 in T Cells Reveals a Pivotal Role of TCRalphabeta+ Intraepithelial Lymphocytes in Preventing Lymphopenia-Associated Colitis. *PLoS One* 10:e0128761.

32 Lohoff, M., Duncan, G. S., Ferrick, D., Mittrucker, H. W., Bischof, S., Prechtl, S., Rollinghoff, M., Schmitt, E., Pahl, A., and Mak, T. W. 2000. Deficiency in the transcription factor interferon regulatory factor (IRF)-2 leads to severely compromised development of natural killer and T helper type 1 cells. *J Exp Med* 192:325.

33 Robinette, M. L., Fuchs, A., Cortez, V. S., Lee, J. S., Wang, Y., Durum, S. K., Gilfillan, S., Colonna, M., and Immunological Genome, C. 2015. Transcriptional programs define molecular characteristics of innate lymphoid cell classes and subsets. *Nat Immunol* 16:306.

34 Califano, D., Cho, J. J., Uddin, M. N., Lorentsen, K. J., Yang, Q., Bhandoola, A., Li, H., and Avram, D. 2015. Transcription Factor Bcl11b Controls Identity and Function of Mature Type 2 Innate Lymphoid Cells. *Immunity* 43:354.

35 Tang, L., Peng, H., Zhou, J., Chen, Y., Wei, H., Sun, R., Yokoyama, W. M., and Tian, Z. 2016. Differential phenotypic and functional properties of liver-resident NK cells and mucosal ILC1s. *J Autoimmun* 67:29.

36 Constantinides, M. G., Gudjonson, H., McDonald, B. D., Ishizuka, I. E., Verhoef, P. A., Dinner, A. R., and Bendelac, A. 2015. PLZF expression maps the early stages of ILC1 lineage development. *Proc Natl Acad Sci U S A* 112:5123.

37 Sato, T., Onai, N., Yoshihara, H., Arai, F., Suda, T., and Ohteki, T. 2009. Interferon regulatory factor-2 protects quiescent hematopoietic stem cells from type I interferon-dependent exhaustion. *Nat Med* 15:696.

38 Pobezinsky, L. A., Etzensperger, R., Jeurling, S., Alag, A., Kadakia, T., McCaughtry, T. M., Kimura, M. Y., Sharrow, S. O., Guinter, T. I., Feigenbaum, L., and Singer, A. 2015. Let-7 microRNAs target the lineage-specific transcription factor PLZF to regulate terminal NKT cell differentiation and effector function. *Nat Immunol* 16:517.

39 Harly, C., Cam, M., Kaye, J., and Bhandoola, A. 2018. Development and differentiation of early innate lymphoid progenitors. *J Exp Med* 215:249.

40 Sun, L., Jiang, Z., Acosta-Rodriguez, V. A., Berger, M., Du, X., Choi, J. H., Wang, J., Wang, K. W., Kilaru, G. K., Mohawk, J. A., Quan, J., Scott, L., Hildebrand, S., Li, X., Tang, M., Zhan, X., Murray, A. R., La Vine, D., Moresco, E. M. Y., Takahashi, J. S., and Beutler, B. 2017. HCFC2 is needed for IRF1- and IRF2-dependent Tlr3 transcription and for survival during viral infections. *J Exp Med* 214:3263.

Figure legends

Figure 1. Intestinal ILC populations in *Irf2*$^{-/-}$ mice.

(A) Flow cytometry analysis of ILCs in the lamina propria in the small intestine in control and *Irf2*$^{-/-}$ mice. Cumulative data representing 5 pairs for NKp46^{+} ILC3, ILC1 and cNK cells and 3 pairs for NKp46^{-}CD4^{+}, NKp46^{-}CD4^{-} ILC3s and ILC2. CD45^{+}CD3^{-}NKp46^{+} cells were examined for NK1.1 and CD127 expression. (B) CD127 and KLRG1 expression on CD45^{+}CD3^{-}NKp46^{-} cells. CD127^{+}KLRG1^{-}NKp46^{-} cells were further examined for CD4 expression. Numbers represent the percentages of cells within the gates and quadrants (A, B). (C) Frequencies (upper) and absolute numbers (lower) of indicated ILC subpopulations in control (open symbols) and *Irf2*$^{-/-}$ (closed symbols) mice. Each population among CD45^{+}CD3^{-} cells is defined as; NKp46^{+}ILC3: NKp46^{+}CD127^{+}NK1.1^{-}, NKp46^{-}CD4^{+}ILC3: KLRG1^{-}CD127^{+}NKp46^{-}CD4^{+}, NKp46^{-}CD4^{-}ILC3: KLRG1^{-}CD127^{+}NKp46^{-}CD4^{-}, ILC2: KLRG1^{+}CD127^{+}, ILC1: NKp46^{+}CD127^{+}NK1.1^{+}, cNK: NKp46^{+}CD127^{-}NK1.1^{+}. Each symbol represents an individual animal. Horizontal lines are the mean. Statistically significant differences are marked: *P<0.05, **P<0.01, ns; not significant.

Figure 2. Small-intestinal ILC populations in *Irf2*$^{-/-}$*Rag1*$^{-/-}$ mice.

(A, B) Flow cytometry analysis of intestinal ILC3 subpopulations (A) and ILC2s (B) in control *Rag1*$^{-/-}$*Rorc*$^{gfp/+}$ and *Irf2*$^{-/-}$*Rag1*$^{-/-}$*Rorc*$^{gfp/+}$ mice. Each ILC population among CD45^{+}CD3^{-} viable cells was defined as; NKp46^{+}ILC3: RORγt^{+}NKp46^{+}, NKp46^{-}CD4^{+}ILC3: RORγt^{+}NKp46^{-}CD4^{+}, NKp46^{-}CD4^{-}ILC3: RORγt^{+}NKp46^{-}CD4^{-}, ILC2: KLRG1^{+}NKp46^{-}, ILC1: RORγt^{-}NKp46^{+}CD127^{+}NK1.1^{+}, cNK: RORγt^{-}NKp46^{+}CD127^{-}NK1.1^{+}. Numbers indicate the percentages of cells within the gates. (C) Frequencies (upper) and absolute numbers (lower) of ILC subpopulations in control *Rag1*$^{-/-}$*Rorc*$^{gfp/+}$ (open symbols) and *Irf2*$^{-/-}$*Rag1*$^{-/-}$*Rorc*$^{gfp/+}$ (closed symbols) mice. Each symbol represents individual animal. Horizontal lines are the mean. Statistically significant differences are marked: *P<0.05, **P<0.01, ns; not significant.

Figure 3. ILC2 precursors (ILC2Ps) in the BM.

(A) Flow cytometry for ILC2Ps (cKit^{-}T1ST2^{+}SCA1^{+}KLRG1^{-}) in the bone marrow in control and *Irf2*$^{-/-}$mice. CD45^{+}Lin^{-} cells were analyzed. The lineage cocktail contained anti-CD25 antibody. (B) Frequencies (left) and absolute numbers (right) of ILC2Ps in control (open symbols) and *Irf2*$^{-/-}$ (closed symbols) mice. Each symbol represents individual animal. Horizontal lines are the mean. Statistically significant differences are marked: *P<0.05, **P<0.01.

Figure 4. ILC populations in the liver and lungs in *Irf2*$^{-/-}$*Rag1*$^{-/-}$ mice.

(A) Flow cytometry analysis of CD45^{+} cells in the liver in control *Rag1*$^{-/-}$ and *Irf2*$^{-/-}$*Rag1*$^{-/-}$mice for cNK cells (NKp46^{+}NK1.1^{+}DX5^{+}CD49a^{-}) and ILC1s (NKp46^{+}NK1.1^{+}DX5^{-}CD49a^{+}). (B) Flowcytometry for cNK cells (NKp46^{+}NK1.1^{+}CD127^{-}), ILC1s (NKp46^{+}NK1.1^{+}CD127^{+}) and ILC2s (NK1.1^{-}NKp46^{-}KLRG1^{+}CD127^{+}) within CD45^{+} cells in the lungs in control *Rag1*$^{-/-}$and *Irf2*$^{-/-}$*Rag1*$^{-/-}$mice. (A, B) Numbers indicate the percentages of cells within the gates. (C) Frequencies (upper) and absolute numbers (lower) of cNK cells and ILCs defined as in A and B in the liver and lungs in control *Rag1*$^{-/-}$ (open symbols) and *Irf2*$^{-/-}$*Rag1*$^{-/-}$ (closed symbols) mice. Each symbol represents individual mouse. Horizontal bars show the mean. Statistically significant differences are marked: *P<0.05, **P<0.01, ns; not significant.

Figure 5. Developing ILC progenitors in the BM in *Irf2*$^{-/-}$ mice.

(A) Absolute numbers of cNK cells and ILCs in the lamina propria in the small intestine, defined as in Fig.1, in h*BCL2*-transgenic (triangles) and nontransgenic (circles) *Irf2*$^{-/-}$*Rag1*$^{-/-}$ mice. NKp46^{-}CD4^{+} and CD4^{-} ILC3 subpopulations were examined

together in this figure. Each symbol represents individual animal. Horizontal bars show the mean. Statistically significant differences are marked: *P<0.05, ns; not significant. (B) CHILPs (cKit^{+}CD127^{+}FLT3^{-}α4β7^{hi}), ILCPs (cKit^{+}CD127^{+}FLT3^{-}α4β7^{hi}PD1^{hi}) and PD1$^{lo/-}$CHILPs (cKit^{+}CD127^{+}FLT3^{-}α4β7^{hi}PD1$^{lo/-}$) in BM CD45^{+}Lin^{-}CD25^{-} cells of control and *Irf2*$^{-/-}$ mice. (C) Frequencies (upper) and absolute numbers (lower) of whole, PD-1^{hi} (ILCPs) and PD-1$^{lo/-}$ CHILPs in control (open symbols) and *Irf2*$^{-/-}$ (closed symbols) mice. Each symbol represents individual animal. Statistically significant differences are marked: *P<0.05, ns; not significant.

Figure 6. PLZF^{hi} subpopulation was missing in CHILPs in *Irf2*$^{-/-}$ mice.

(A) Intracellular staining for PLZF in CHILPs (cKit^{+}CD127^{+}α4β7^{+}) in control and *Irf2*$^{-/-}$ mice. CD45^{+}Lin^{-}CD25^{-} BM cells were analyzed. (B) Frequencies of PLZF^{hi} cells among PD-1^{hi} CHILPs defined as in (A). Open and closed symbols represent control and *Irf2*$^{-/-}$ mice, respectively. Each symbol represents individual animal. **P<0.01. (C) Quantitative RT-PCR for *Zbtb16* messages in CLP (cKit^{+}CD127^{+}FLT3^{+}α4β7^{-}), CHILPs (cKit^{+}CD127^{+}FLT3^{-}α4β7^{+}) and PD-1^{hi} CHILPs sorted from CD45^{+}Lin^{-}CD25^{-} BM cells from control (open columns) and *Irf2*$^{-/-}$ (filed columns) mice. Data represent the means and SD of RT-PCR trials for 3 independent sortings for CLPs and PD-1^{hi} CHILPs

and 2 independent sortings for whole CHILPs. (D) Quantitative RT-PCR for *Irf2* messages in CLPs, whole CHILPs and PD-1^{hi} CHILPs sorted as in C from the BM of control mice, representing the means and SD of 3 independent sortings. (C, D) Statistically significant differences are marked: **P<0.01, ns; not significant. (E) Flowcytometry for PLZF in immature (NK1.1^{-}) and mature (NK1.1^{+}) developing iNKT cells, defined as TCRβ^{dull} cells binding CD1d dimers loaded with αGalCer, in control (open histograms) and *Irf2*$^{-/-}$ (filed histograms) thymi.

Figure 1

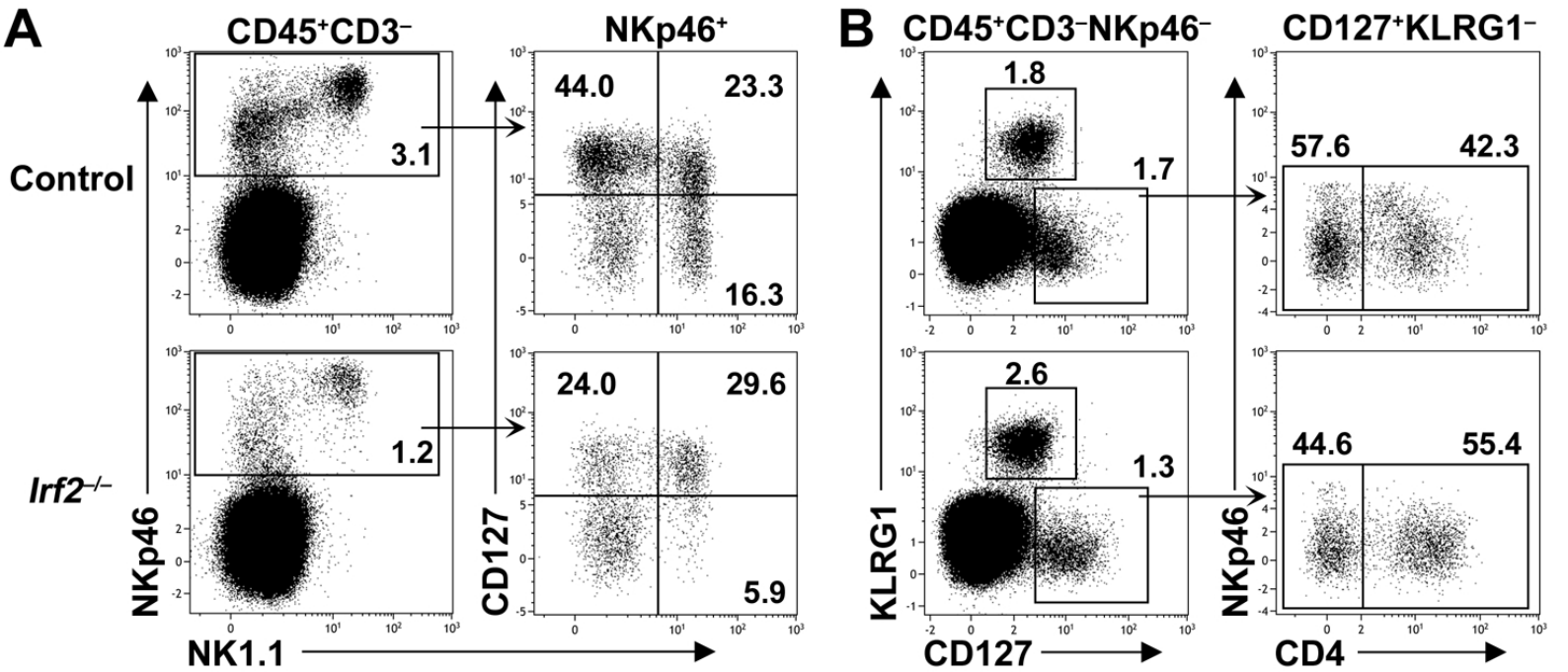
A
CD45+CD3−
NKp46+
Control
Irf2−/−
3.1
44.0
23.3
16.3
1.2
24.0
29.6
5.9
NKp46
NK1.1
CD127
B
CD45+CD3−NKp46−
CD127+KLRG1−
1.8
1.7
57.6
42.3
2.6
1.3
44.6
55.4
KLRG1
CD127
NKp46
CD4

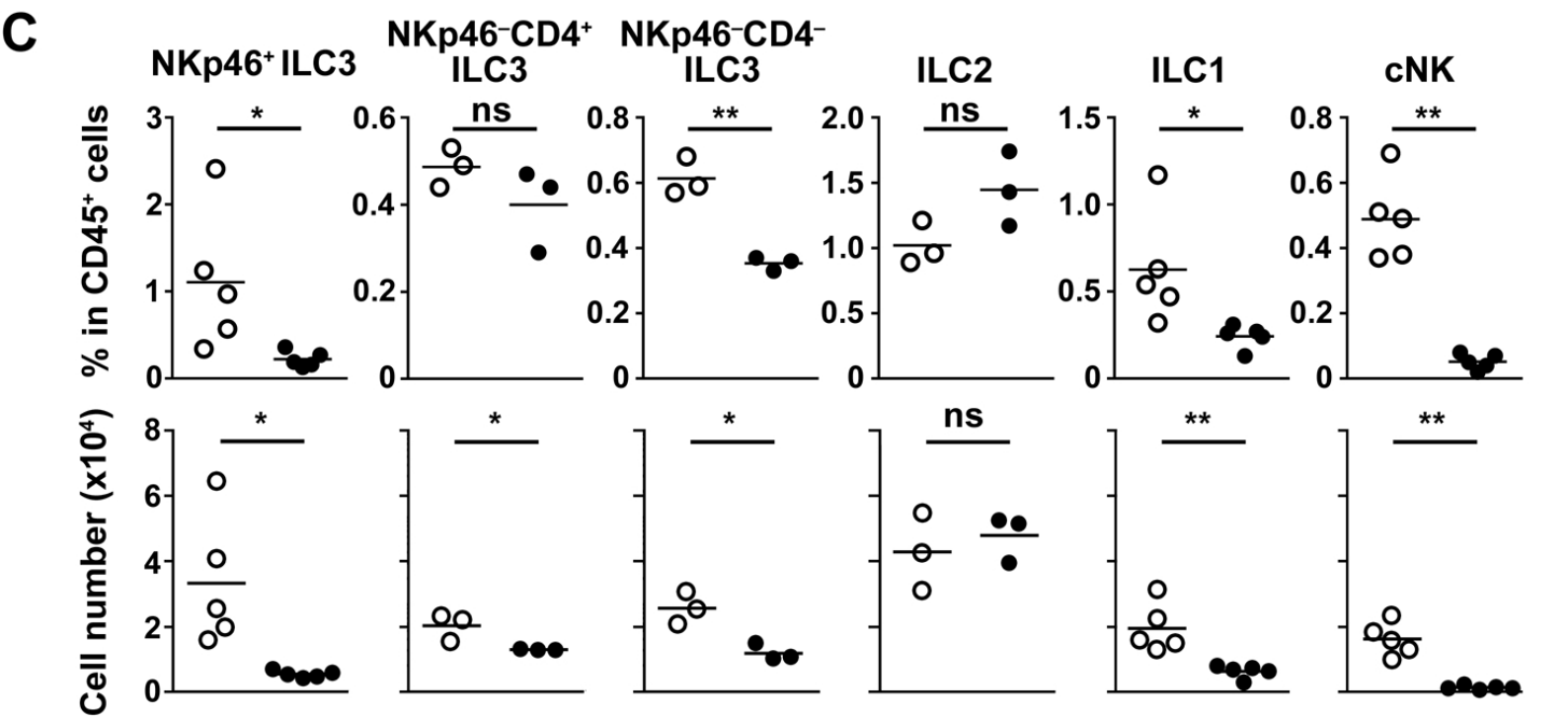
C
NKp46+ ILC3
NKp46−CD4+ ILC3
NKp46−CD4− ILC3
ILC2
ILC1
cNK
% in CD45+ cells
Cell number (x10⁴)
*
ns
**

Figure 2

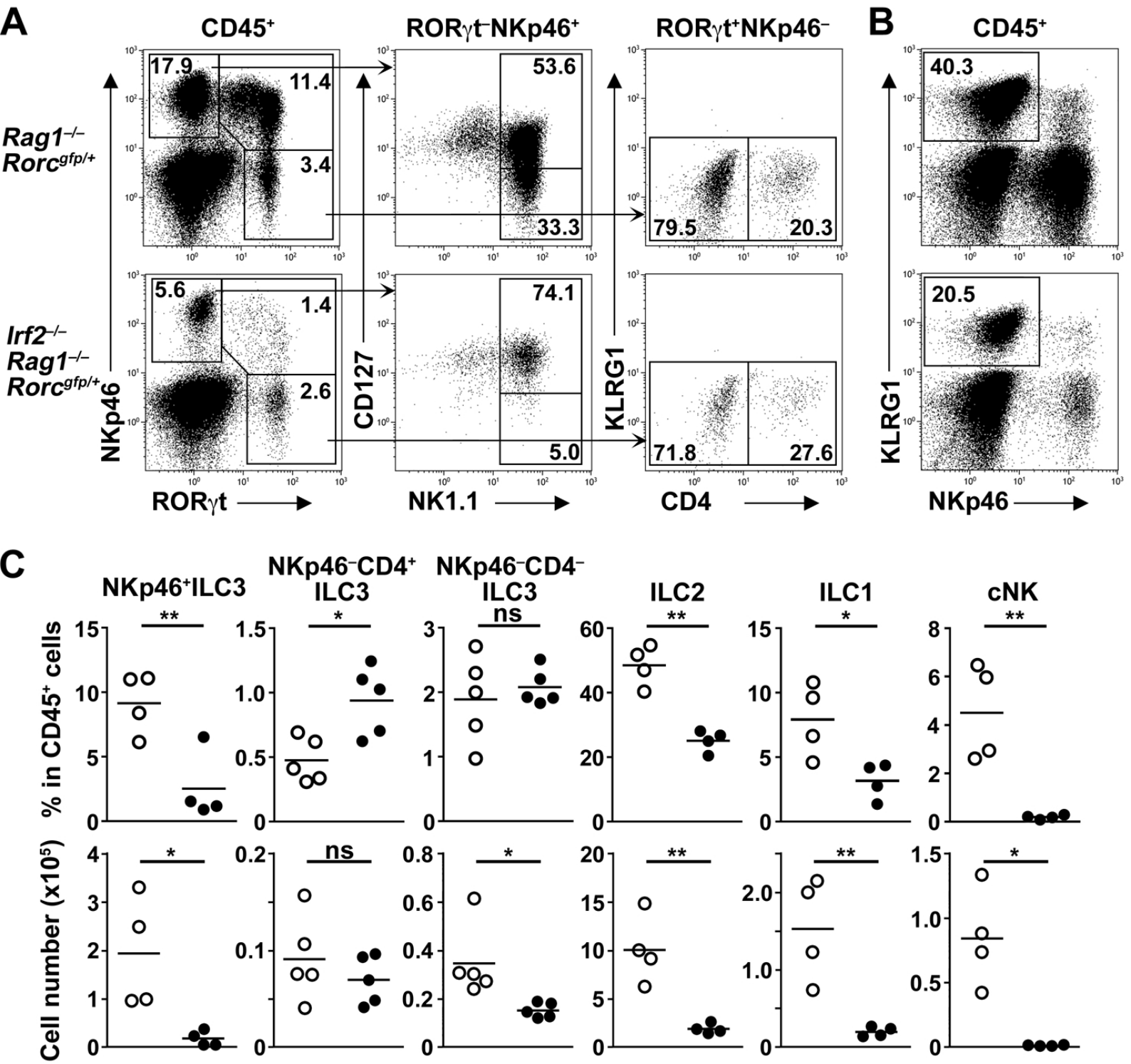
A
CD45+
RORγt−NKp46+
RORγt+NKp46−
Rag1−/− Rorcgfp/+
Irf2−/− Rag1−/− Rorcgfp/+
17.9
11.4
3.4
53.6
33.3
79.5
20.3
5.6
1.4
2.6
74.1
5.0
71.8
27.6
NKp46
RORγt
CD127
NK1.1
KLRG1
CD4
B
CD45+
40.3
20.5
KLRG1
NKp46
C
NKp46+ILC3
NKp46−CD4+ ILC3
NKp46−CD4− ILC3
ILC2
ILC1
cNK
% in CD45+ cells
Cell number (x10⁵)
**
*
ns

Figure 3

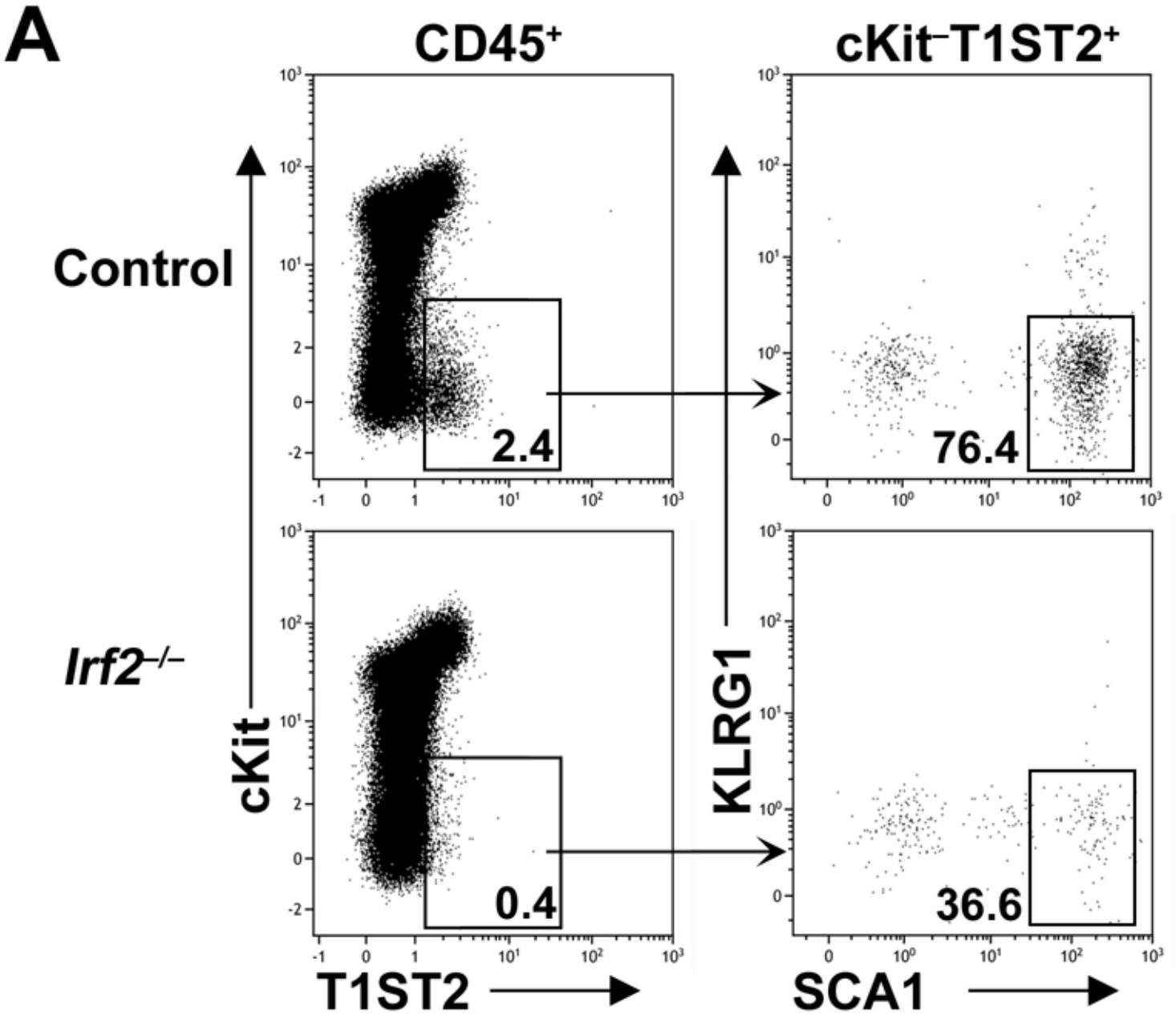
A
CD45+
cKit–T1ST2+
Control
Irf2–/–
2.4
76.4
0.4
36.6
cKit
T1ST2
KLRG1
SCA1

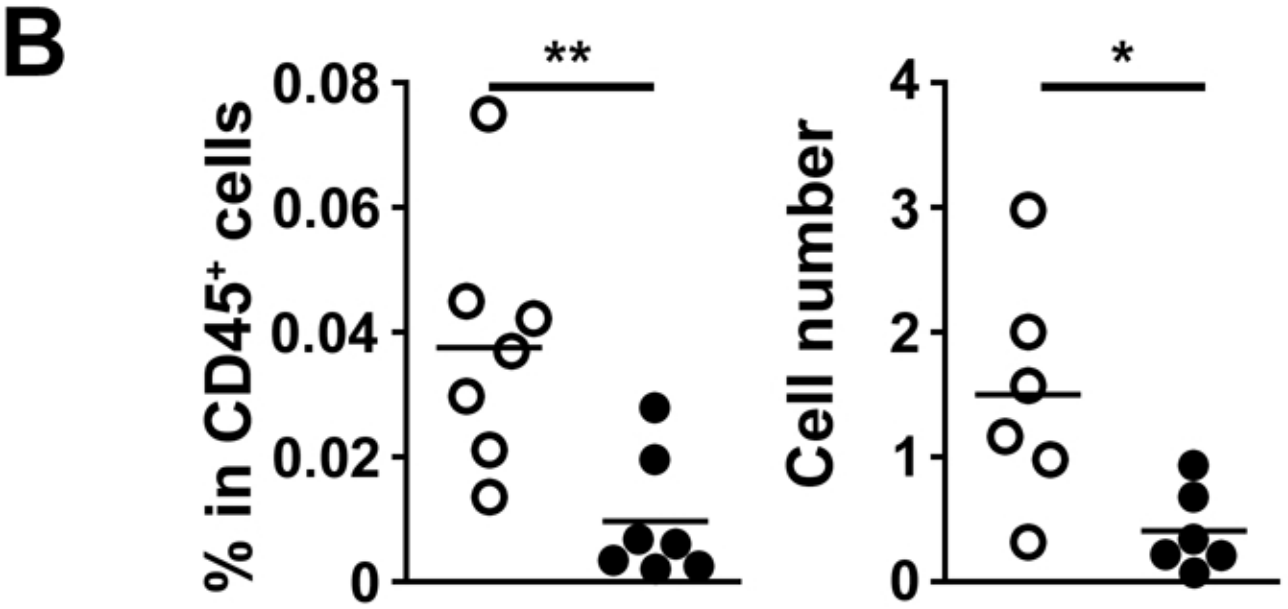
B
**
*
% in CD45+ cells
Cell number
0.08
0.06
0.04
0.02
0
4
3
2
1
0

Figure 4

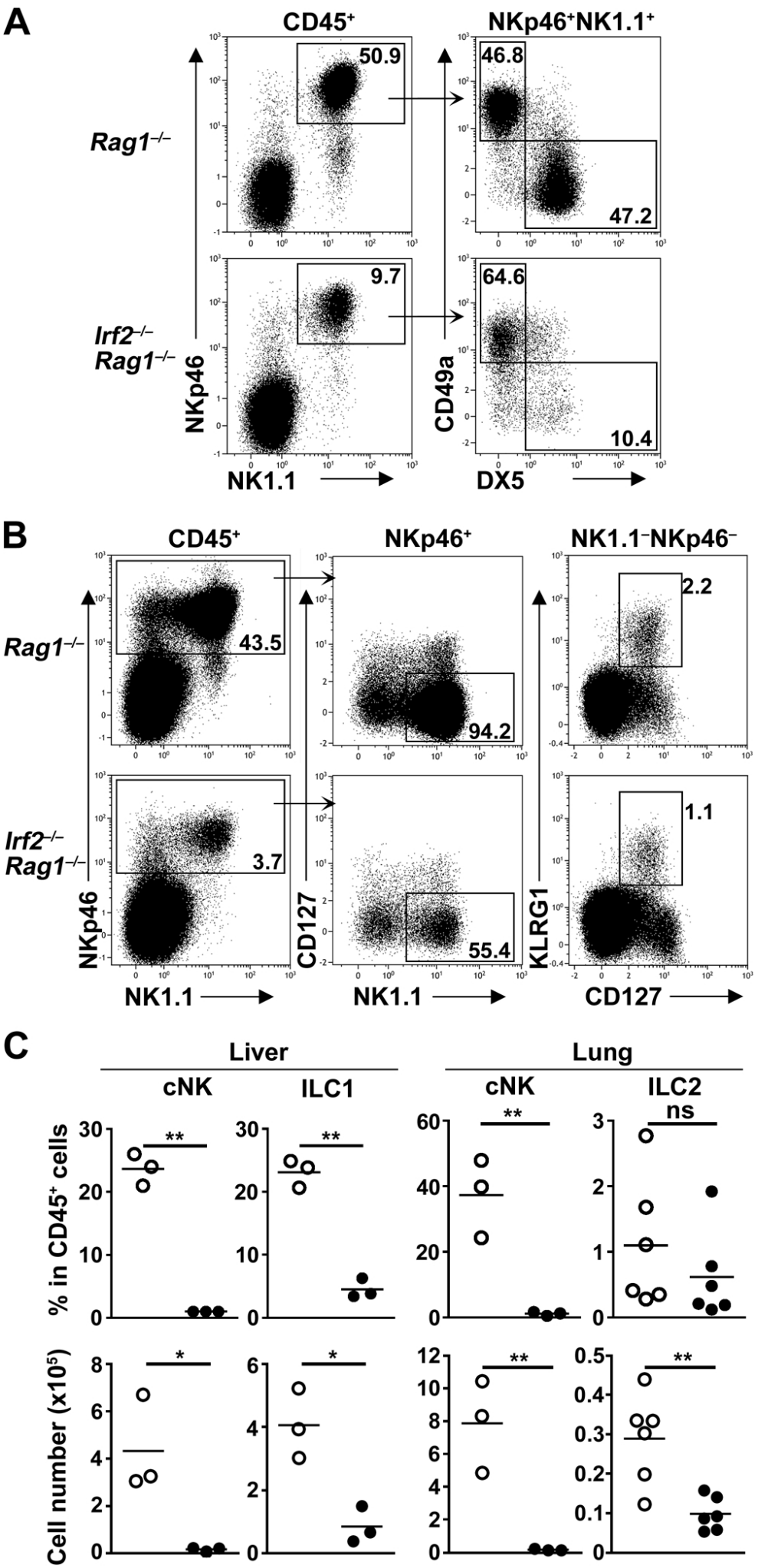
A
CD45+
NKp46+NK1.1+
Rag1−/−
Irf2−/− Rag1−/−
50.9
46.8
47.2
9.7
64.6
10.4
NKp46
NK1.1
CD49a
DX5
B
CD45+
NKp46+
NK1.1−NKp46−
Rag1−/−
Irf2−/− Rag1−/−
43.5
94.2
2.2
3.7
55.4
1.1
NKp46
NK1.1
CD127
NK1.1
KLRG1
CD127
C
Liver
Lung
cNK
ILC1
cNK
ILC2
ns
% in CD45+ cells
Cell number (x10⁵)

Figure 5

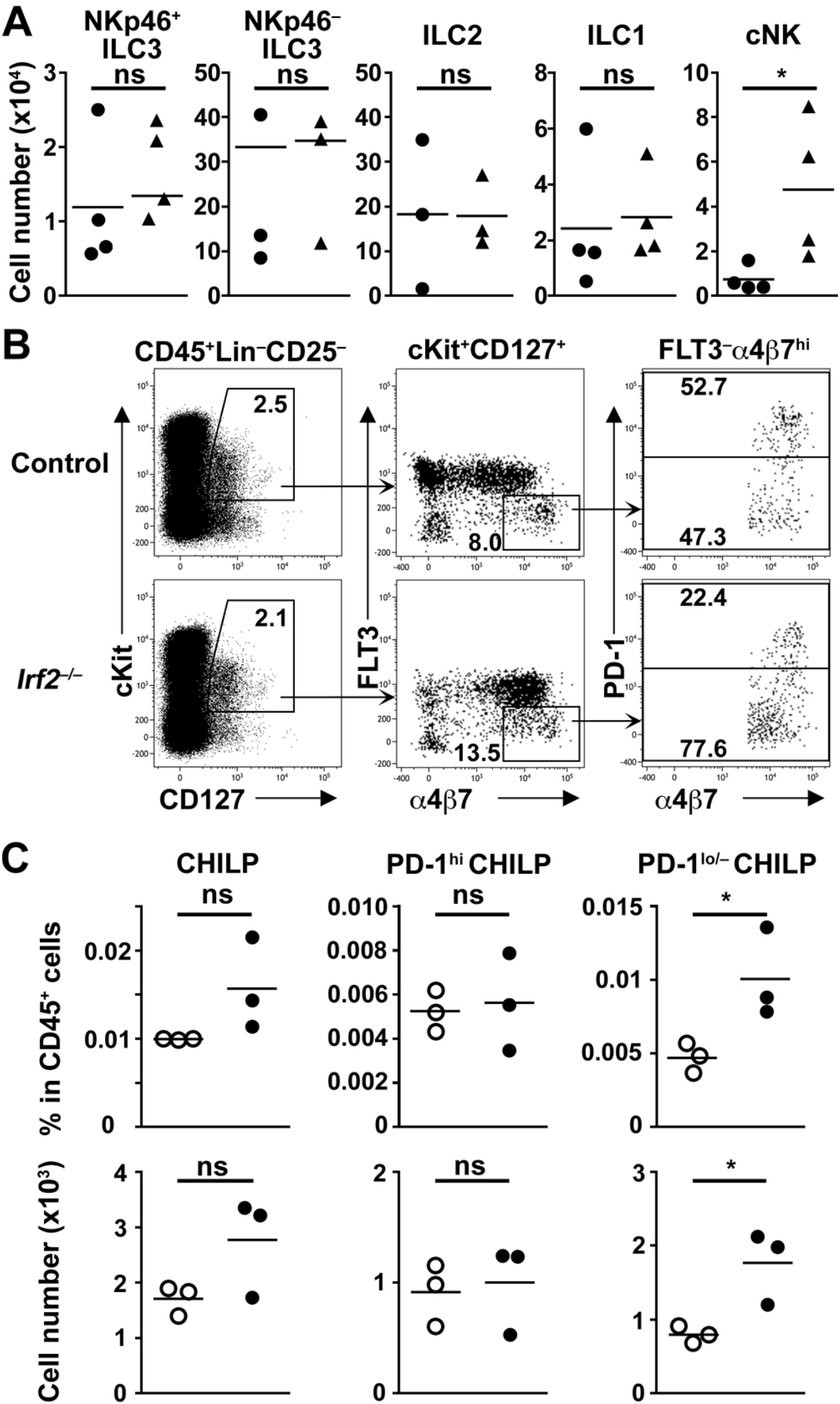
A
NKp46+ ILC3
NKp46– ILC3
ILC2
ILC1
cNK
ns
ns
ns
ns
*
Cell number (x10⁴)
B
CD45+Lin–CD25–
cKit+CD127+
FLT3–α4β7hi
Control
Irf2–/–
2.5
2.1
8.0
13.5
52.7
47.3
22.4
77.6
cKit
CD127
FLT3
α4β7
PD-1
α4β7
C
CHILP
PD-1hi CHILP
PD-1lo/– CHILP
ns
ns
*
% in CD45+ cells
Cell number (x10³)
ns
ns
*

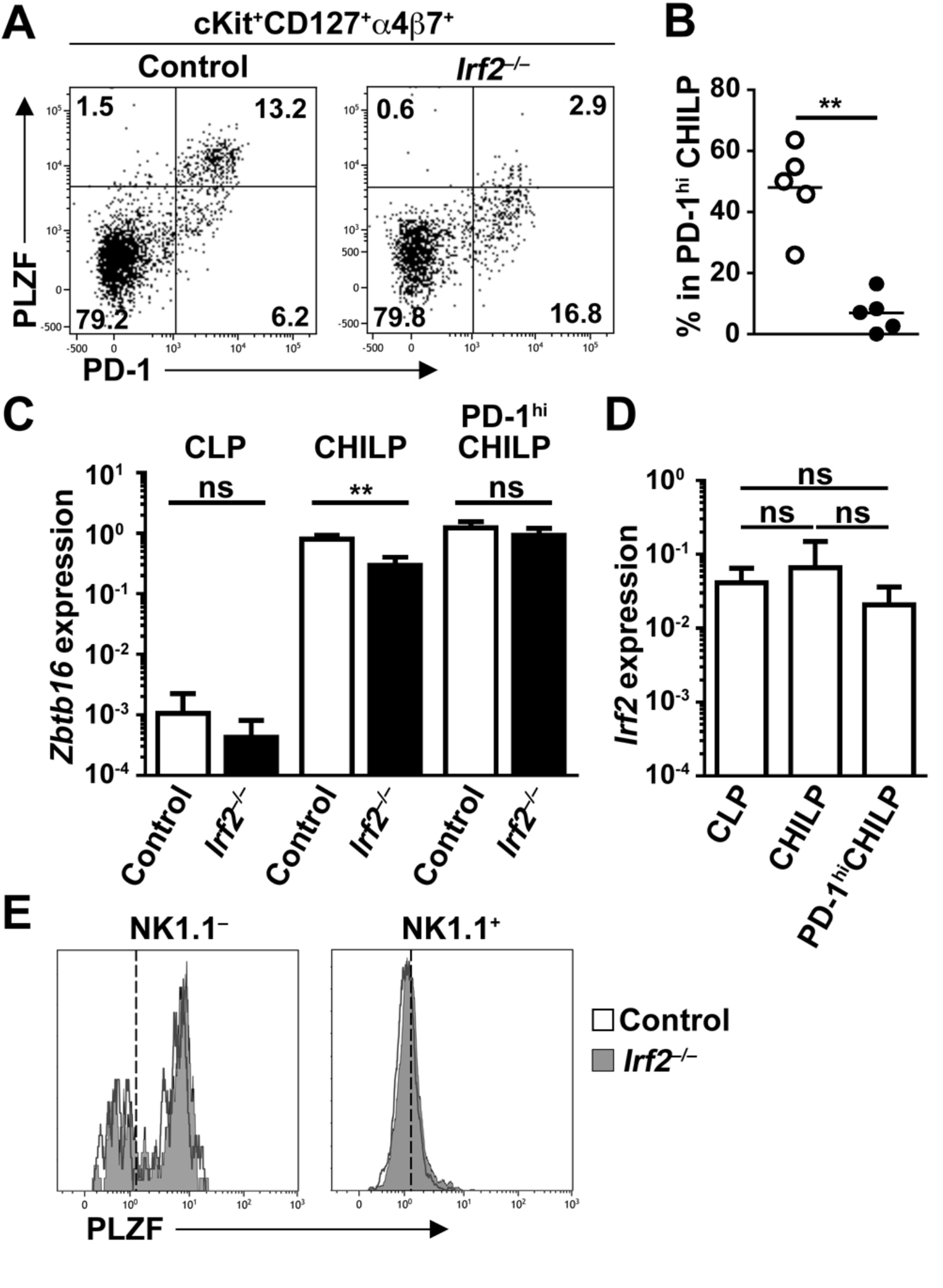
A
cKit+CD127+α4β7+
Control
Irf2−/−
1.5
13.2
79.2
6.2
0.6
2.9
79.8
16.8
PLZF
PD-1
B
% in PD-1hi CHILP
**
C
CLP
CHILP
PD-1hi CHILP
Zbtb16 expression
ns
**
ns
Control
Irf2−/−
D
Irf2 expression
ns
ns
ns
CLP
CHILP
PD-1hiCHILP
E
NK1.1−
NK1.1+
PLZF
Control
Irf2−/−

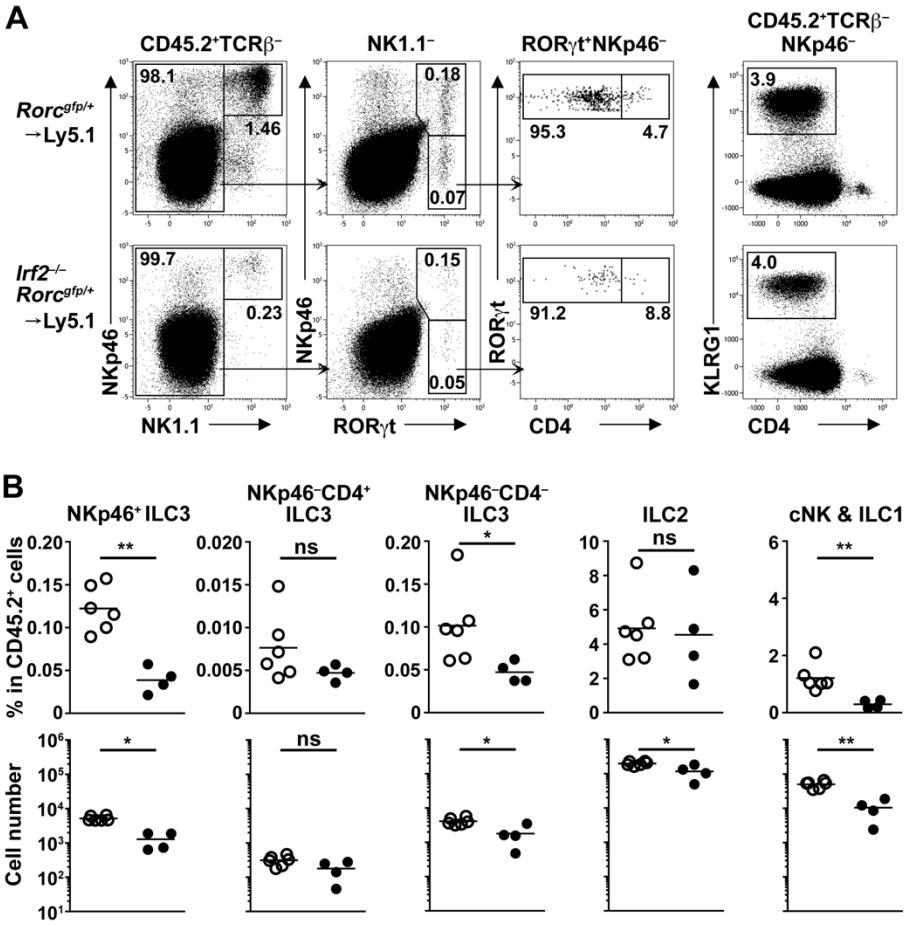

Supplementary Figure 1. Cell-intrinsic requirement for IRF-2 in ILC development.

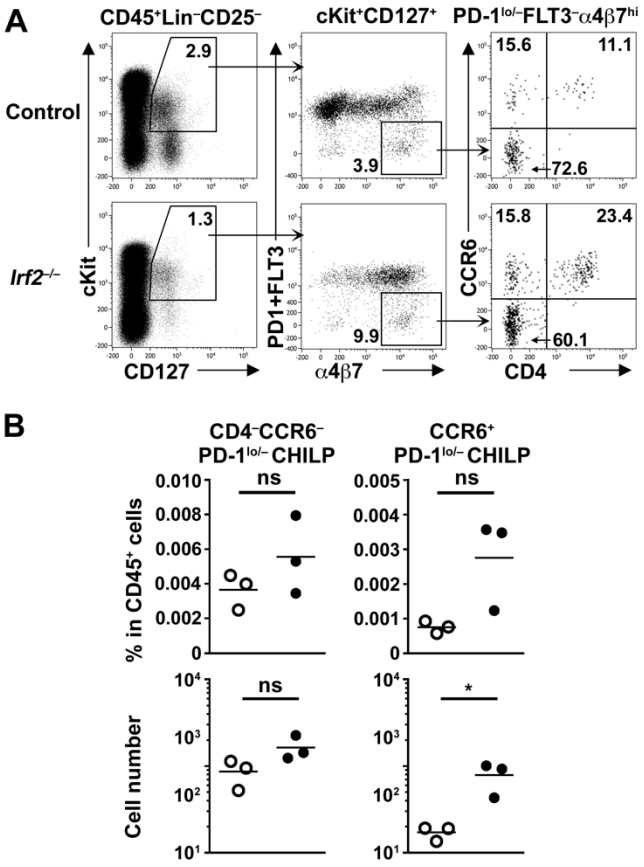

Supplementary Figure 2. Deviation of early ILC development towards LTi-like cell lineage.

Legends for Suplementary figures

Figure S1

(A) Bone marrow cells from control *Rorc*$^{gfp/+}$ or *Irf2*$^{-/-}$*Rorc*$^{gfp/+}$ mice were transferred into irradiated B6-Ly5.1 mice. CD45.2^{+} donor-derived ILCs in the small-intestinal lamina propria in those chimeric mice were analyzed by flow cytometry. Numbers indicate the percentages of cells within the gates. (B) Frequencies (upper) and absolute numbers (lower) of CD45.2^{+} donor-derived NKp46^{+} ILC3 (RORγt^{+}NKp46^{+}NK1.1^{-}), NKp46^{-}CD4^{+} ILC3 (RORγt^{+}NKp46^{-}NK1.1^{-}CD4^{+}), NKp46^{-}CD4^{-} ILC3 (RORγt^{+}NKp46^{-}NK1.1^{-}CD4^{-}), ILC2 (NKp46^{-}KLRG1^{+}), ILC1+cNK (NKp46^{+}NK1.1^{+}) as analyzed in (A). Each symbol represents individual chimeras. Statistically significant differences are marked: *P<0.05, **P<0.01, ns; not significant.

Figure S2

(A) Flowcytometry for PD-1$^{lo/-}$ CHILP (cKit^{+}CD127^{+}FLT3^{-}α4β7^{hi}PD-1$^{lo/-}$). These cells were further examined for CCR6^{-}CD4^{-} and CCR6^{+} subpopulations. CD45^{+}Lin^{-}CD25^{-} cells were analyzed. Note that FLT3^{+} and PD-1^{+} populations were gated out together (middle panels). (B) Frequencies (upper) and absolute numbers (lower) of CD4^{-}CCR6^{-} and CCR6^{+}PD-1$^{lo/-}$ CHILPs in control (open symbols) and *Irf2*$^{-/-}$ (closed symbols) mice. Each symbol represents individual animal. Statistically significant differences are marked: *P<0.05, ns; not significant.